The Journal of Neuroscience, September 1, 1999, *19*(17):7342–7355

Junctional versus Extrajunctional Glycine and $GABA_A$ Receptor-Mediated IPSCs in Identified Lamina I Neurons of the Adult Rat Spinal Cord

Nadège Chéry and Yves De Koninck

Department of Pharmacology and Therapeutics, McGill University, Montréal, Québec, H3G 1Y6 Canada

Colocalization of GABA and glycine in synaptic terminals of the superficial dorsal horn raises the question of their relative contribution to inhibition of different classes of neurons in this area. To address this issue, miniature IPSCs (mIPSCs) mediated via $GABA_A$ receptors ($GABA_A$Rs) and glycine receptors (GlyRs) were recorded from identified laminae I-II neurons in adult rat spinal cord slices. $GABA_A$R-mediated mIPSCs had similar amplitude and rise times, but significantly slower decay kinetics than GlyR-mediated mIPSCs. Lamina I neurons appeared to receive almost exclusively GlyR-mediated mIPSCs, even after application of hypertonic solutions. Yet, all neurons responded to exogenous applications of both GABA and glycine, indicating that they expressed both $GABA_A$Rs and GlyRs. Given that virtually all glycinergic interneurons also contain GABA, the possibility was examined that $GABA_A$Rs may be located extrasynaptically in lamina I neurons. A slow $GABA_A$R-mediated component was revealed in large, but not minimally evoked monosynaptic IPSCs. Administration of the benzodiazepine flunitrazepam unmasked a $GABA_A$R component to most mIPSCs, suggesting that both transmitters were released from the same vesicle. The isolated $GABA_A$R component of these mIPSCs had rising kinetics 10 times slower than that of the GlyR component (or of $GABA_A$R mIPSCs in lamina II). The slow $GABA_A$R components were prolonged by GABA uptake blockers.

It is concluded that, whereas GABA and glycine are likely released from the same vesicle of transmitter in lamina I, $GABA_A$Rs appear to be located extrasynaptically. Thus, glycine mediates most of the tonic inhibition at these synapses. This differential distribution of $GABA_A$Rs and GlyRs confers distinct functional properties to inhibition mediated by these two transmitters in lamina I.

Key words: dorsal horn; substantia gelatinosa; nociception; miniature IPSCs; slice; inhibition

The superficial laminae I and II of the dorsal horn play a pivotal role in the integration and relay of pain-related information (Perl, 1984; Willis, 1985; Light, 1992; Craig, 1996), and thus elucidating the nature of inhibitory control in this area is crucial for our understanding of nociceptive processing. Both GABA and glycine function as inhibitory neurotransmitters in the mammalian spinal cord (for review, see Todd and Spike, 1993), and blocking either of these control mechanisms produces a hypersensitivity characteristic of neuropathic pain syndromes (Yaksh, 1989; Sivilotti and Woolf, 1994; Sherman and Loomis, 1996; Sorkin and Puig, 1996). Previous studies report the coexistence of GABA and glycine as well as their respective receptors at many synapses in the superficial dorsal horn of the rat spinal cord (van den Pol and Gorcs, 1988; Bohlhalter et al., 1994, 1996; Todd et al., 1995, 1996), and it appears that nearly all glycine-immunoreactive cells in this area are also GABA-immunoreactive (although only half of GABAergic cells contain glycine) (Todd and Sullivan, 1990; Mitchell et al., 1993). Recent evidence indicates the possible co-storage of GABA and glycine within the same vesicles at some synapses (Burger et al., 1991; Christensen and Fonnum, 1991; Chaudhry et al., 1998; Jonas et al., 1998). These findings raise the question of whether both transmitters are contained within the same synaptic vesicles, co-released, and act together at the same synaptic junction in the superficial dorsal horn, and therefore whether they play distinct roles in inhibition of laminae I and II neurons.

Previous studies focused on $GABA_A$ and glycine receptor-mediated inhibition in lamina II of the spinal dorsal horn (Yoshimura and Nishi, 1995) or trigeminal medulla (Grudt and Williams, 1994). They did not directly address the question of co-release from the same vesicles, nor whether inhibition mediated by GABA and glycine differed among identified classes of neurons, in part because they did not identify lamina I neurons. Thus, data are lacking on this layer that represents one of the main spinal nociceptive output pathways (Willis, 1989; Light, 1992; Craig, 1994).

Recordings from lamina I in slices have remained limited by the difficulty to maintain and delineate this thin layer in conventional preparations. To overcome this, we used a parasagittal slice of adult rat spinal cords that respects the natural rostrocaudal orientation of marginal layer neurons (Light et al., 1979; Woolf and Fitzgerald, 1983; Lima and Coimbra, 1986; De Koninck et al., 1992), thus allowing visual identification of lamina I (Chéry and De Koninck, 1997; De Koninck and Chéry, 1998) while still providing visual access to deeper layers. Using this approach, we performed whole-cell patch-clamp recordings in identified spinal laminae I-II neurons to study spontaneously occurring miniature

Received Feb. 8, 1999; revised June 21, 1999; accepted June 22, 1999.

This work was supported by National Institute for Neurological Disorders and Stroke Grant NS 34022 and by Canadian Medical Research Council (MRC) Grant MT 12170 to Y.D.K. Y.D.K. is a Scholar of the Canadian MRC. N.C. was the recipient of a Faculty of Medicine Graduate Award and an Eileen Peters McGill Major Fellowship. We thank Drs. R. Čapek, M. W. Salter, and A. J. Todd for helpful comments on this manuscript and Ms. A. Constantin for expert technical assistance. We thank Hoffman-La Roche for the generous donation of flunitrazepam and Abbott Labs for tiagabine.

Correspondence should be addressed to Dr. Yves De Koninck, Department of Pharmacology and Therapeutics, McGill University, 3655 Drummond, #1317, Montreal, Quebec, H3G 1Y6 Canada.

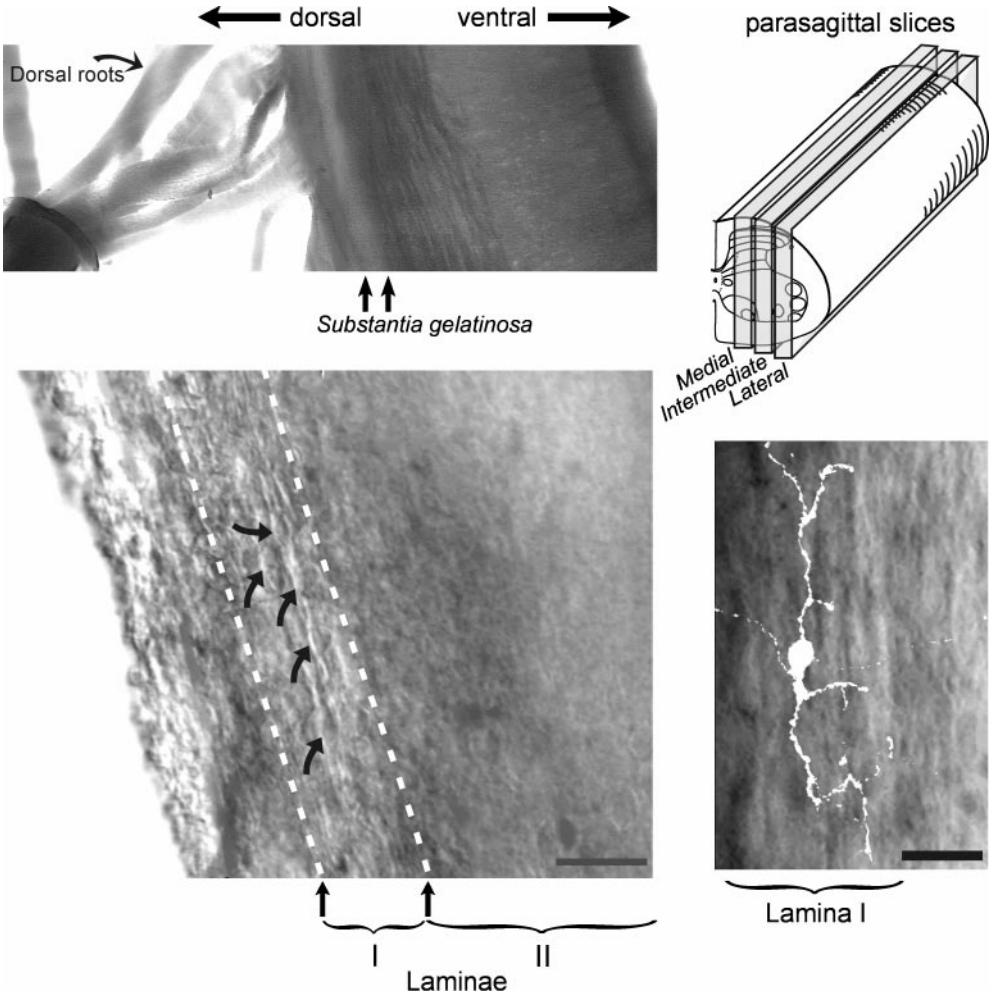

Figure 1. Visualization of the dorsal horn and delineation of laminae I and II in parasagittal 400-μm-thick slices of the spinal cord. The low-power micrograph at the top (*left*) illustrates a portion of the slice with dorsal rootlets attached. Note the clear band (*arrows*) corresponding to the *substantia gelatinosa* (lamina II). On the *right* side is a schematic drawing of the parasagittal plane of slicing, illustrating the lateral, intermediate, and medial slices that can be obtained. The micrograph at the bottom (*left*) is a high-power image of the superficial layers viewed with infrared differential interference contrast (IR-DIC) under a Zeiss Axioscope. *Arrows* point to distinctive lamina I neurons. Note the distinctive striated appearance of lamina I, which allows us to delineate it from lamina II. The micrograph on the *right* side shows a higher power image of lamina I on which is superimposed a confocal reconstruction of a lamina I neuron that was filled with Lucifer yellow during the recording. Note the typical rostrocaudal orientation of the dendritic tree of these neurons with their dendrites mainly confined to lamina I (rostral is *up*, caudal is *down*).

(action potential-independent) IPSCs (mIPSCs) that are thought to reflect transmitter release from single vesicles.

An important initial finding was that lamina I neurons were almost exclusively bombarded by glycine receptor (GlyR)-mediated mIPSCs even though all cells appeared to express both $GABA_A$ receptors ($GABA_A$Rs) and GlyRs, suggesting that perhaps $GABA_A$Rs were not located at synaptic junctions in this layer. To test this hypothesis more directly, we manipulated release, receptor sensitivity, and uptake system using electrical stimulation, benzodiazepines, and GABA uptake inhibitors. The results are consistent with the interpretation that $GABA_A$Rs are likely located at extrasynaptic sites in lamina I.

Some of these results have been reported in preliminary form (Chéry and De Koninck, 1997; Chéry and De Koninck, 1998).

MATERIALS AND METHODS

Slice preparation. Adult male Sprague Dawley rats (30- to 60-d-old) were anesthetized with Na^+ pentobarbital (30 mg/kg) and perfused intracardially for 15–20 sec with ice-cold oxygenated (95% O_2 and 5% CO_2) sucrose-substituted ACSF (S-ACSF) containing (in mM): 252 sucrose, 2.5 KCl, 2 $CaCl_2$, 2 $MgCl_2$, 10 glucose, 26 $NaHCO_3$, 1.25 NaH_2PO_4, and 5 kynurenic acid, pH 7.35; 340–350 mOsm. The rats were then rapidly decapitated, and the spinal cord was immediately removed by hydraulic extrusion and immersed in ice-cold S-ACSF for 1–2 min. In some cases, a laminectomy was performed before the perfusion for subsequent surgical extraction of the cord rather than by hydraulic extrusion. Lumbar and cervical segments (2-cm-long) were isolated and glued, lateral side down, on a brass platform with cyanoacrylate cement, in a chamber filled with oxygenated ice-cold S-ACSF, and 400-μm-thick parasagittal sections were cut. The slices were then incubated in S-ACSF at room temperature (23–28°C) for 30 min and subsequently transferred to a storage chamber filled with oxygenated normal ACSF (126 mM NaCl instead of sucrose, 300–310 mOsm) at room temperature. After a minimum incubation of 1 hr, the slices were transferred to a recording chamber under a Zeiss Axioscope equipped with infrared differential interference contrast (IR-DIC) and water immersion-objectives for visualization of neurons in thick live tissue. The slices were perfused at ~2 ml/min with oxygenated ACSF containing the glutamate receptor antagonists 6-cyano-7-nitroquinoxaline-2,3-dione (CNQX, 10 μM; Tocris Cookson, Bristol, UK), and D-2-amino-5-phosphonovaleric acid (D-AP-5; 40 μM; Tocris Cookson). All recordings were performed at room temperature.

Labeling and reconstruction of neurons. All neurons were labeled during the recordings by including Lucifer yellow (dipotassium salt, 0.5–1%; Sigma, St. Louis, MO) in the recording pipette. Simple diffusion of the dye from the pipette into the cell during the course of the recording was sufficient to obtain complete labeling. Immediately after the end of the recording, the slice was placed between wet filter paper to prevent wrinkling and fixed by immersion in 4% paraformaldehyde in 0.1 M phosphate buffer. Subsequently, the slices were cryoprotected by infiltration with 30% sucrose in 0.1 M phosphate buffer, overnight at 4°C, and processed later for confocal light microscopy. The slices were examined under a Zeiss LSM 410 inverted laser scanning microscope equipped with argon/krypton and helium/neon lasers. From 40–60 serial optical sections (1 μm apart) of the Lucifer yellow-labeled cell were obtained. With this approach, it was possible to reconstruct the entire dendritic tree and perform three-dimensional rotations in different planes for full morphological identification of each neuron.

Drug application. Bicuculline methiodide (10 μM; Research Biochemicals, Natick, MA), SR-95531 (3 μM; Research Biochemicals) and strychnine hydrochloride (100 nM to 1 μM; Research Biochemicals) were added

to the ACSF from frozen, aliquoted stock solutions. For recording of action potential-independent mIPSCs, 1 μM tetrodotoxin (TTX; Research Biochemicals) was added to the bathing solution. GABA and glycine were prepared similarly and dissolved in ACSF containing 10 mM HEPES in replacement for the bicarbonate buffer, to reach a concentration of 1 mM. These amino acids were applied locally onto lamina I-II dorsal horn neurons by pressure ejection through glass micropipettes. Two pipettes, connected to a two-channel Picospritzer, were positioned close to the cells and contained GABA and glycine, respectively, except in control experiments in which one of the pipettes contained only vehicle solution. In some cases, GABA and glycine were bath-applied. In experiments aimed at forcing additional vesicle release, pressure-application of hypertonic ACSF onto the recorded neurons was used (sucrose was added to HEPES-buffered ACSF to obtain an osmolarity of 590–610 mOsm). In some experiments, to potentiate possible subliminal $GABA_A$R-mediated events, the benzodiazepine flunitrazepam (Hoffman-La Roche, Basel, Switzerland) was bath-applied (1 μM). The GABA uptake blockers tiagabine (25–50 μM; Abbott Labs, Irving, TX) and 1-(2-(((Diphenylmethylene)imino)oxy)ethyl)-1,2,5,6-tetrahydro-3-pyridine-caboxylic acid hydrochloride (NO-711; 10–30 μM; Research Biochemicals) were also used to study accumulation of synaptically released GABA.

Whole-cell recording and data acquisition. For whole-cell voltage-clamp recordings, patch pipettes were pulled from borosilicate glass capillaries (with an inner filament, WPI) using a two-stage vertical puller (PP-83; Narishige, Tokyo, Japan). The pipettes were filled with an intracellular solution composed of (in mM): 140 CsCl, 10 HEPES, 2 $MgCl_2$, and 0.5% Lucifer yellow (Sigma). The pH was adjusted to 7.2 with CsOH, and the osmolarity ranged from 260–280 mOsm (pipette resistance, 3 MΩ). In >80% of the recordings, we added 2 mM ATP, 0.4 mM GTP, 11 mM BAPTA (all from Sigma), and 1 mM $CaCl_2$ to the intracellular solution. Recordings were obtained by lowering the patch electrode onto the surface of visually identified neurons in lamina I or II. Neurons with a healthy appearance presented a smooth surface, and the cell body and parts of the dendrites could be clearly seen. These neurons also had fusiform or oval cell bodies (usually 10–20 μm in length). Neurons with round, swollen cell bodies were avoided because recording from them revealed low resting membrane potential and poor membrane integrity. While monitoring current responses to 5 mV pulses, a brief suction was applied to form >1GΩ seals. An Axopatch 200B amplifier (Axon Instruments, Foster City, CA) with >80% series resistance compensation was used for the recording. The access resistance was monitored throughout each experiment. Only recordings with access resistance between 7 and 20 MΩ (average 14 ± 1 MΩ; mean ± SEM) were considered acceptable for analysis of IPSCs, and only recording with stable access throughout the entire administration of antagonists were used for classification of $GABA_A$R- and GlyR-mediated IPSCs. Traces were low-pass filtered at 10 kHz and stored on a videotape, using a digital data recorder (VR-10B, Instrutech Corp.). Off-line, the recordings were low-pass filtered at 2–3 kHz and sampled at 10–20 kHz, on an Intel Pentium-based computer using the Strathclyde Electrophysiology software (CDR; by J. Dempster, Department of Physiology and Pharmacology, University of Strathclyde, Glasgow, UK).

Eliciting monosynaptic IPSCs and detection of spontaneous IPSCs. Monosynaptic $GABA_A$R- and GlyR-mediated IPSCs were evoked by electrical stimulation via either bipolar tungsten electrodes for large intensity stimuli, or a patch micropipette for focal stimulations. Square-wave constant pulses (200–300 μsec duration) were applied at a frequency of ≤0.3 Hz. The electrode was placed within 20–50 μm of the neuron cell body (for proximal stimuli) or within 20–50 μm of a distal branch of a dendrite at 150–300 μm away from the soma (for distal stimulation) along the bipolar axis of the dendritic tree of lamina I neurons. Individual spontaneously occurring IPSCs (sIPSCs and mIPSCs) were detected off-line using a software trigger as previously described (De Koninck and Mody, 1994). For each experiment, the detected events were examined; any noise that spuriously met the trigger specifications was rejected. For analysis of the decay phase of sIPSCs or mIPSCs, the events were selected on the basis of the following criteria: (1) traces containing multiple events were discarded and (2) only events that had stable baselines before the rise and after the end of the decay were kept for analysis. Rise times were determined between 10 and 90% of the peak amplitude of the IPSCs. For averaging of IPSCs, the events were software aligned by their initial rising phase. All software for analysis was designed by Y. De Koninck.

Statistical analysis and curve fitting. Peak amplitudes, rise times, and decay time constants were calculated for each of several hundreds of sIPSCs or mIPSCs per cell, using an automated algorithm (De Koninck and Mody, 1994, 1996). Averages of several hundred mIPSC were also superimposed for comparison. Decay time constants were fitted using a least square method based on a simplex algorithm as previously described (De Koninck and Mody, 1994). The goodness of fit was evaluated on the basis of fitting subsets of points drawn from the whole set of data points as well as from evaluation of the reduced χ^2: $\chi^2_\nu = \chi^2/\nu$, where the factor $\nu = N - n$ is the number of degrees of freedom left after fitting N data points to the n parameters. The necessity to introduce additional exponential components to the fits was judged first on the basis of visual inspection of the fitted curves superimposed onto the data. When the merit of additional components was not obvious, an F test was used to assess how the additional component improved the value of the reduced χ^2: $F_\chi = \Delta\chi^2/\chi^2_\nu$ ($df_1 = 1$ and $df_2 = \nu$). The critical value for the merit of additional components was set at a low level ($p < 0.01$) to favor parsimony of the fitted function. When focusing on comparisons of the late component of mIPSCs, fits were started at a fixed interval after the peak of the event to allow for nonequivocal monoexponential fits that provide an easier and fairer reference when dealing with nonaveraged, individual traces (De Koninck and Mody, 1994; Williams et al., 1998). This also avoided contamination of the values of decay time constants with variable weighting factors. Membrane time constants were estimated in voltage-clamp mode from analysis of current transients following 5 mV, 200-msec-long voltage pulses (Rall, 1969; Jackson, 1992; Spruston and Johnston, 1992).

Student t tests, were used to analyze the differences between parameters of the $GABA_A$R- and GlyR-mediated IPSCs. ANOVA was used to determine the differences in rise times of proximally versus distally evoked IPSCs, and *post hoc* tests were obtained with Bonferroni or Tukey corrections. To evaluate the relationship between different parameters, we used the Pearson correlation matrix, and the significance of the r value was determined with an ANOVA followed by at t test using a Bonferroni correction. χ^2 tests for contingency tables were performed to determine the correlation between the laminar location of the cells and the presence of $GABA_A$R- and GlyR-mediated sIPSCs. The critical value for statistical significance was set at $p < 0.05$. All the data are expressed as mean ± SEM, unless otherwise indicated.

RESULTS

Recordings from identified laminae I and II neurons

With our slice preparation, laminae I and II were easily identified. Lamina I neurons had a distinct rostrocaudal orientation (Light et al., 1979; Woolf and Fitzgerald, 1983; Lima and Coimbra, 1986; De Koninck et al., 1992; Ma et al., 1996; Zhang et al., 1996; Zhang and Craig, 1997) and appeared densely packed (Fig. 1). Most of the cells in lamina I had a bipolar morphology in the parasagittal plane, with rostrocaudal dendritic arborization (Fig. 1), but a few neurons with dendrites extending dorsally and/or ventrally could also be clearly identified. The cell bodies in lamina I were usually small (5–20 μm in length, in the longitudinal axis). Lamina II neurons, in contrast, had larger cell bodies (20–50 μm in length). Consistent with previous reports, the thickness of lamina I ranged from 15 to 50 μm (Ribeiro-da-Silva, 1995; Todd et al., 1998), being closer to 20 μm in the medial slices, whereas the more lateral sections had thicker lamina I because of the curving of the superficial layers at the lateral border of the dorsal horn (Fig. 1). The recorded lamina I neurons were at an average distance of 10 ± 2 μm from the dorsal border between the gray and white matter, indicating that these neurons clearly belonged to the marginal layer (Fig. 1). In contrast, the recorded lamina II neurons were located at an average distance of 67 ± 9 μm from the dorsal border of the gray matter to ensure a clear distinction between the sample of cells belonging to these two laminae.

Differential distribution of $GABA_A$R- and GlyR-mediated mIPSCs in laminae I-II neurons

Spontaneous mIPSCs were observed in 322 of 387 recorded laminae I-II neurons of the dorsal horn, in the presence of 10 μM

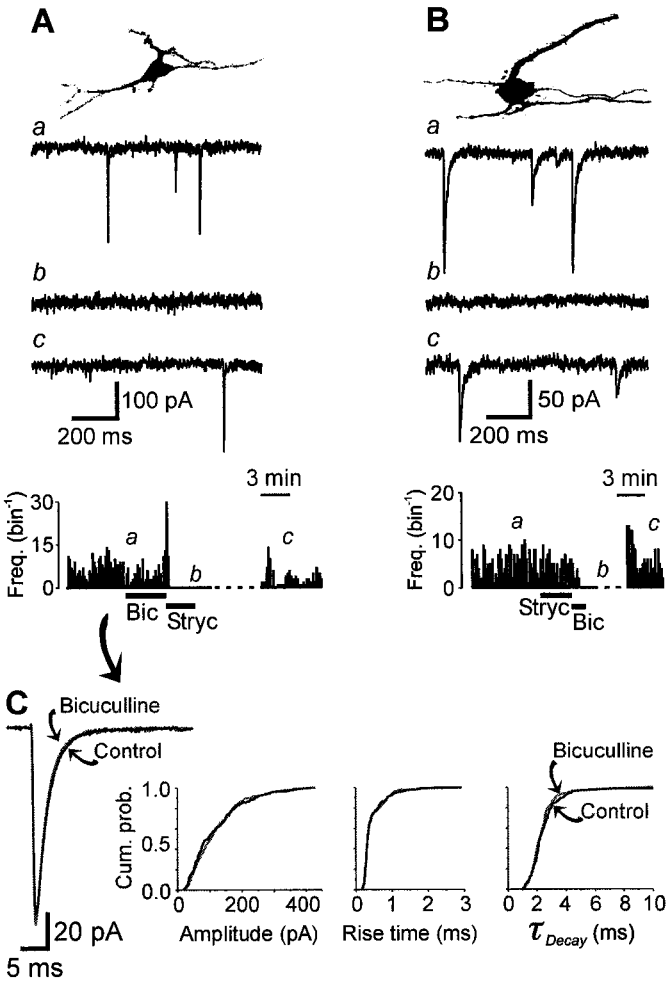

Figure 2. $GABA_A$R- and GlyR-mediated mIPSCs occur in distinct populations of neurons in the superficial laminae. The *top* micrographs in *A* and *B* illustrate confocal reconstructions of these lamina II neurons in the parasagittal plane (dorsal is *up*, rostral is to the *right*). Note the more stellar orientation of the dendritic tree of these cells in contrast to the lamina I neuron illustrated in Figure 1. *A*, GlyR-mediated mIPSCs are selectively blocked by strychnine. The raw traces are representative examples of GlyR-mediated mIPSCs taken at points indicated on the time histogram at the bottom (bin width, 10 sec). The mean frequency was not significantly altered after bath application of 10 μM bicuculline (0.74 sec^{-1} vs 0.65 sec^{-1}), but 100 nM strychnine completely blocked all the events. *B*, $GABA_A$R-mediated mIPSCs are selectively blocked by bicuculline. Representative traces are examples of $GABA_A$R-mediated mIPSCs taken at points indicated on the time histogram at the *bottom* (bin width, 10 sec). *C*, The amplitude and kinetics parameters of the GlyR-mediated mIPSCs recorded in *A* were not altered after bath application of 10 μM bicuculline. The cumulative probability plots show the lack of change in the distributions of amplitude, 10–90% rise time, and decay time constant (τ_{Decay}) after bicuculline administration (mean amplitude, -110 ± 13 pA vs -130 ± 14 pA; $p > 0.1$; mean rise time, 0.27 vs 0.24 msec; $p > 0.5$; mean decay time constant (τ_D), 2.24 vs 2.21 msec; $p > 0.5$). The *inset* on the *left* shows superimposed averages of 228 and 289 consecutive mIPSCs before and after addition of bicuculline, respectively. Similarly for $GABA_A$R-mediated mIPSCs, they were not affected by up to 1 μM strychnine (data not shown; mean amplitude, -79 ± 12 pA vs -69 ± 15 pA; $p > 0.1$; mean rise time, 0.71 vs 0.84 msec; $p > 0.1$; mean decay time constant, 11.19 vs 12.33 msec; $p > 0.5$). Thus, GABA and glycine mediate separate mIPSCs in laminae I-II neurons. The holding membrane potential was −65 mV.

CNQX, 40 μM APV and 1 μM TTX, with a recording time varying from 2 to 90 min. To determine whether these miniature events were mediated by activation of $GABA_A$Rs or GlyRs, we used the selective $GABA_A$R antagonists bicuculline (10 μM) or SR-95531 (3 μM) and the GlyR antagonist strychnine (100 nM; Fig. 2). For a comparison of the distribution of $GABA_A$R- and GlyR-mediated mIPSCs, only data from 51 neurons (31 in lamina I and 20 in lamina II) were retained, because (1) the recordings were of sufficient duration, (2) the access resistance was stable throughout the testing of antagonists, and (3) it was possible to test the effects of both bicuculline (or SR-95531) and strychnine. Almost all lamina I neurons (30 of 31) displayed mIPSCs that could be entirely, selectively, and reversibly abolished by 100 nM strychnine, indicating that they were mediated by glycine (Table 1). In contrast, 11 of the 20 neurons in lamina II received exclusively SR-95531- or bicuculline-sensitive mIPSCs, suggesting that they were mediated via activation of $GABA_A$Rs (Fig. 2*B*); the remaining neurons in lamina II displayed exclusively strychnine-sensitive mIPSCs, indicating their mediation by glycine (Fig. 2*A*, Table 1). None of the cells tested in laminae I and II displayed both GlyR- and $GABA_A$R-mediated mIPSCs together. In cells with GlyR-mediated mIPSCs (that were selectively blocked by 100 nM strychnine; Fig. 2*A*) administration of 10 μM bicuculline or 3 μM SR-95531 did not decrease the frequency of events (Fig. 2*A*) or affect their amplitude, rise times, and decay kinetics ($n = 34$; $p > 0.2$; paired comparisons; Fig. 2*C*). To test for the possibility that, in these cases, bicuculline might have decreased the frequency of the events by an undetectable amount (i.e., a very small proportion of the events might have been GABAergic), in some experiments we added 100 nM strychnine first, and in all cases it completely blocked all of the mIPSCs ($n = 5$). Conversely, in cells with GABAergic mIPSCs, the synaptic events were selectively abolished by 10 μM bicuculline (Fig. 2*B*), although up to 1 μM strychnine failed to affect these synaptic events or decrease their frequency ($n = 12$; $p > 0.2$; Fig. 2*B*). These findings indicate that mIPSCs have distinct distributions in laminae I-II neurons.

Additional experiments were performed in the absence of TTX to record spontaneous IPSCs (sIPSCs; $n = 9$). As for mIPSCs, virtually all of these sIPSCs were also completely blocked by strychnine in lamina I. Thus, results with sIPSCs were pooled with those from mIPSCs (Table 1).

Using our recording technique, no apparent run down of either type of mIPSCs was observed, even with recordings lasting >2 hr as we previously reported in other tissues in absence of ATP or additional calcium buffers in the recording pipettes (De Koninck and Mody, 1994, 1996; Otis et al., 1994). Nevertheless, because of the possibility that some $GABA_A$R-mediated currents may be more sensitive to the lack of ATP and calcium buffering (Chen et al., 1990; however, see De Koninck and Mody, 1996), after the initial recordings, we always added 2 mM ATP, 0.4 mM GTP, 11

Table 1. Differential distribution of $GABA_A$R- and GlyR-mediated spontaneous IPSCs (pooled sIPSCs with mIPSCs) in laminae I and II neurons of the dorsal horn

	GlyR	$GABA_A$R	Total
Lamina I	39	1	40
Lamina II	9	11	20
Total	48	12	60

$\chi^2 = 19.80$; degree of freedom = 1; $p < 0.001$.

Table 2. Summary of the properties of $GABA_A$R- and GlyR-mediated mIPSCs recorded in laminae I-II neurons of the dorsal horn (expressed as mean ± SEM)

	Peak amplitude (pA)	Frequency (Hz)	Rise time (μs)	Decay time constant (msec)	Input resistance (MΩ)	Access resistance (MΩ)
Glycinergic	87.5 ± 6.1	1.0 ± 0.2	403 ± 36	5.8 ± 0.3	422 ± 69	13.9 ± 1.1
GABAergic	72.9 ± 10.3	0.6 ± 0.2	455 ± 64	10.5 ± 0.6*	544 ± 240	14.0 ± 1.8

*$p < 0.001$.

mM BAPTA, and 1 mM $CaCl_2$ to the intracellular solution for all subsequent recordings. We found no difference in the recordings obtained with the two different intracellular solutions; thus all the data were pooled.

Distinct kinetic properties of $GABA_A$R- and GlyR-mediated mIPSCs

Miniature IPSCs mediated by GlyRs in lamina I had amplitude and kinetic properties that were not different from those in lamina II and therefore were pooled for comparison with properties of $GABA_A$R-mediated mIPSCs recorded in lamina II.

A number of parameters were similar for both GlyR- and $GABA_A$R-mediated mIPSCs. Their frequency was variable with an average of 1.0 ± 0.2 Hz (range, 0.1–5.0 Hz; $n = 19$) for GlyR mIPSCs, and an average frequency of 0.6 ± 0.2 Hz (range, 0.1–1.8 Hz; $n = 17$) for $GABA_A$R mIPSCs. The difference in frequency was not significant between these two populations of mIPSCs ($p > 0.05$; Table 2). In all cases, the mIPSCs amplitude distribution was skewed. The mean amplitude of GlyR-mediated events was 87.5 ± 6.1 pA ($n = 30$). The $GABA_A$R-mediated mIPSCs had a mean amplitude of 72.9 ± 10.3 pA ($n = 11$), not significantly different from that of GlyR-mediated mIPSCs (Fig. 3, Table 2). Similarly, the average 10–90% rise time for $GABA_A$R-mediated mIPSCs was comparable to that of GlyR-mediated events (455 ± 64 μsec vs 403 ± 36 μsec, respectively; $p > 0.5$).

The decay time course of $GABA_A$R-mediated mIPSCs was however significantly slower than that of GlyR-mediated mIPSCs (Fig. 3, Table 2). For quantitative comparison, the decay phase of individual mIPSCs were fit by a monoexponential function (De Koninck and Mody, 1994, 1996; Williams et al., 1998). Figures 3*Ab* and 3*Bb* illustrate the difference in kinetics of the two populations of mIPSCs. The mean decay time constant (τ_D) of GlyR-mediated mIPSCs was 5.8 ± 0.3 msec versus 10.5 ± 0.6 msec for $GABA_A$R-mediated mIPSCs ($p < 0.001$). The average τ_D at +40 mV were 19.4 ± 1.0 msec for the GlyR-mediated mIPSCs against 25.9 ± 2.4 msec for $GABA_A$R-mediated mIPSCs, respectively ($p < 0.05$). Figure 3 illustrates representative distributions of the rise time, decay time constant, and amplitude of GlyR- and $GABA_A$R-mediated mIPSCs, respectively. The average access resistances during the recordings of $GABA_A$R- and GlyR-mediated inhibitory events were equivalent (14.0 ± 1.8 MΩ vs 13.9 ± 1.1 MΩ, respectively). No correlation

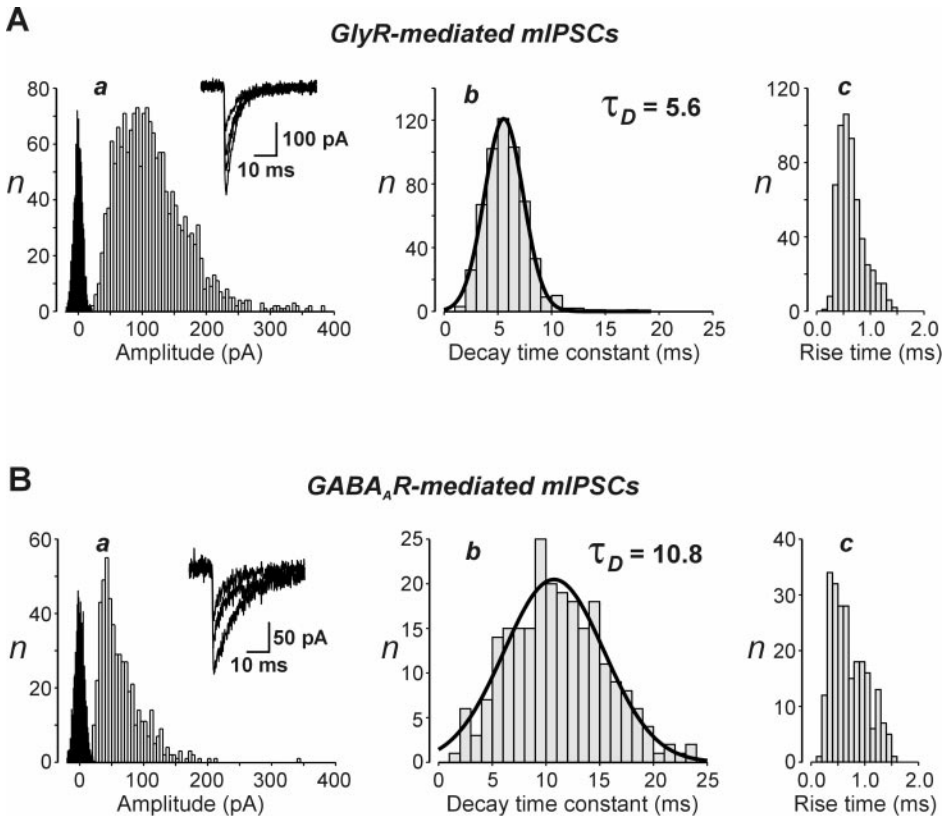

Figure 3. Distinct properties of $GABA_A$R- and GlyR-mediated mIPSCs in laminae I-II neurons. Comparison of the peak amplitudes and kinetic properties of GlyR (*A*) and $GABA_A$R-mediated (*B*) mIPSCs in two different cells. Amplitude distribution of GlyR-mediated (*Aa*) and $GABA_A$R-mediated (*Ba*) mIPSCs (*empty bars, bin width 5 pA*) and corresponding noise distribution (*black bars, bin width 0.5 pA*); in both cells the mIPSCs amplitude distributions are skewed. The *insets* are superimposed representative traces of GlyR mIPSCs (*Aa*) and $GABA_A$R mIPSCs (*Ba*) recorded at −65 mV. The GlyR mIPSCs were specifically blocked by 0.1 μM strychnine and not affected by 10 μM bicuculline (data not shown), whereas 1 μM strychnine did not affect the $GABA_A$R-mediated mIPSCs, which were selectively blocked by 10 μM bicuculline (data not shown). The mean amplitude of the GlyR-mediated mIPSCs in this cell was −111 pA, occurring at a frequency of 5.1 Hz, whereas the mean amplitude of $GABA_A$R-mediated mIPSCs in the other cell (*B*) was −70 pA with a frequency of 1.8 Hz. *Ab, Bb*, Distribution of the decay time constant of GlyR- and $GABA_A$R-mediated mIPSCs, respectively. In both cells, the decays of the mIPSCs were normally distributed (bin width, 1 msec). *Ac, Bc*, The mean 10–90% rise time of GlyR-mediated mIPSCs was 560 μsec, against 630 μsec for the $GABA_A$R-mediated mIPSCs (bin width, 100 μsec). The main difference between these two types of mIPSCs was their decay time course.

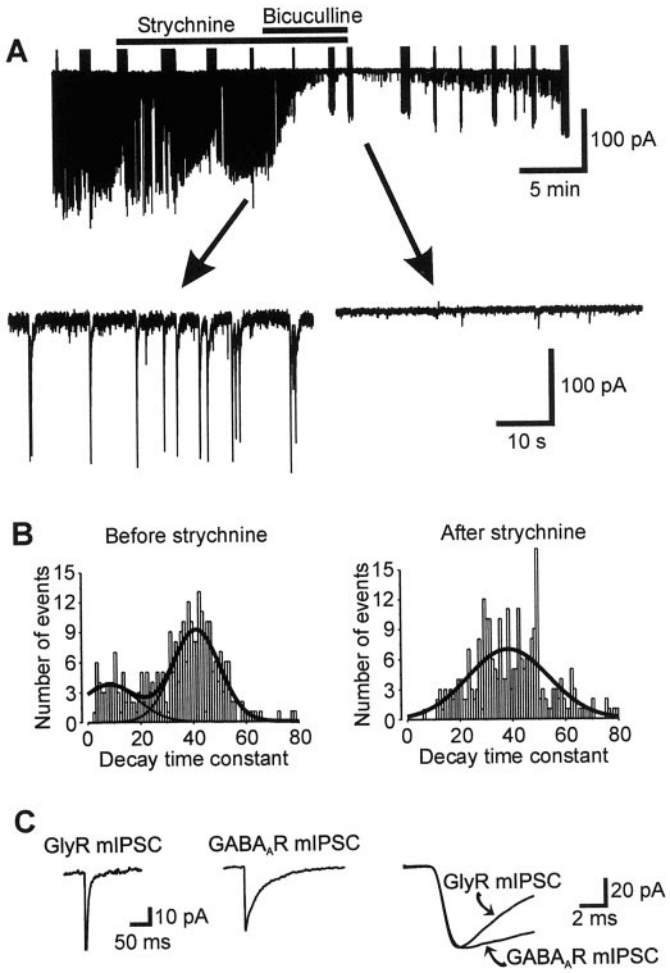

Figure 4. Separate $GABA_A$R- and GlyR-mediated mIPSCs within the same deep dorsal horn neuron. The trace in *A* is a continuous record showing the occurrence of spontaneous mIPSCs over 40 min of recording. Note the periodical testing of the access resistance to the cell (upward and downward dark areas) to ensure that changes in mIPSC amplitude or kinetics is not caused by an increase in series resistance. Strychnine (100 nM) and bicuculline (10 μM) were added to the bathing solution as indicated by the *horizontal bars* above the trace. Although strychnine did not appear to block the mIPSCs on this time scale, bicuculline reversibly blocked the large, slow mIPSCs (see expanded traces below). In *B*, closer inspection of the mIPSC kinetics revealed a heterogeneous population of decays, which were best fitted by the sum of two Gaussians. The group of faster decays disappeared after administration of strychnine, indicating the presence of two populations of mIPSCs in this neuron: GlyR-mediated mIPSCs and slower $GABA_A$R-mediated mIPSCs. The traces in *C* represent averages of 25 mIPSCs automatically selected by computer for decay time constants of <20 msec (*left*) or >20 msec (*right*), thus illustrating the difference in kinetics of the two populations of mIPSCs. The rise times of each group of mIPSCs were not significantly different (0.8 ± 0.2 vs 0.9 ± 0.5 msec, respectively). Thus, $GABA_A$R- and GlyR-mediated mIPSCs can be found within the same cell, but with distinct kinetics.

was found between the access resistance and the rise times for each type of mIPSC ($r = 0.236$; $p > 0.2$). In addition, the input resistance of the neurons displaying $GABA_A$R-mediated mIPSCs was not different from that of cells showing GlyR-mediated mIPSCs (544 ± 240 MΩ vs 422 ± 69 MΩ; respectively, $p > 0.5$). Finally, we found no correlation between the rise time and decay values of miniature $GABA_A$R- and GlyR-mediated events ($r = 0.335$; $p > 0.4$), indicating that the differences in decay time constants could not be accounted for by differences in electrotonic distance from the soma for these two types of mIPSCs (i.e., $GABA_A$R- mediated mIPSCs are unlikely to occur at synapses further away from the soma than GlyR-mediated mIPSCs).

Co-occurrence of both $GABA_A$R- and GlyR-mediated mIPSCs in deeper neurons

Because miniature synaptic currents are thought to reflect release from single vesicles of transmitters, they can serve as a useful tool to test whether GABA and glycine are contained within the same vesicle. For example, if individual mIPSCs included both a $GABA_A$R- and GlyR-mediated component, it could indicate co-packaging of GABA and glycine. In the neurons tested in laminae I and II, the mIPSCs were completely blocked by either strychnine or bicuculline/SR-95531. This cannot rule out the possibility of co-packaging because it may be a consequence of selective expression of one of the two respective receptors in these cells. Because there is clearer evidence that the same cell in lamina III expressed $GABA_A$R and GlyRs (many dendrites in lamina I-II do not belong to laminae I-II cells) (Todd et al., 1996), we recorded mIPSCs in deeper (lamina III) dorsal horn neurons ($n = 5$; Fig. 4). In these cells, two populations of mIPSCs were identified on the basis of their decay kinetics (distribution of decay time constants best fitted by two Gaussians; Fig. 4*B*). After administration of strychnine or bicuculline, only one of the two Gaussian populations of decay time constant remained; for example, in Figure 4, the faster mIPSCs were blocked by application of strychnine. No mIPSC with the combined fast and slow kinetics were found, indicating that separate populations of $GABA_A$R- and GlyR-mediated mIPSCs were found within the same cell. This indicated that, for these cells, either GABA and glycine were likely released from separate vesicles of transmitter or that $GABA_A$Rs and GlyRs were clustered at separate synaptic junctions.

Responses to exogenous applications of GABA and glycine

To determine whether the fact that GABA- and glycine-mediated mIPSCs were never observed jointly within the same cell was caused by a differential expression of their respective postsynaptic receptors among laminae I-II neurons, GABA and glycine were locally applied by pressure ejection to 27 cells. Interestingly, all neurons tested responded to both GABA and glycine (1 mM) regardless of the type of mIPSCs they displayed. Figure 5 illustrates examples of responses induced by application of GABA and glycine in cells showing either exclusively GlyR- or exclusively $GABA_A$R mIPSCs. GABA- and glycine-induced currents could be blocked by bicuculline/SR-95531 or strychnine, respectively (Fig. 5*B–D*), indicating that the responses to these agonists involved receptors similar to those mediating the mIPSCs.

Hypertonic solution-induced release of inhibitory neurotransmitters

To test whether the lack of detection of either $GABA_A$R- or GlyR-mediated mIPSCs reflected a low-frequency of release of one of the two transmitter, in some experiments we applied hypertonic ACSF (590–610 mOsm, adjusted with sucrose) onto laminae I-II neurons ($n = 14$). The hypertonic stress appears to provoke exocytosis of the releasable pool of vesicles and thus substitutes for the calcium-induced release following action potential invasion (Rosenmund and Stevens, 1996). Yet, as the frequency of the synaptic events was increased but remained nonsynchronized, it was still possible to continue recording spon-

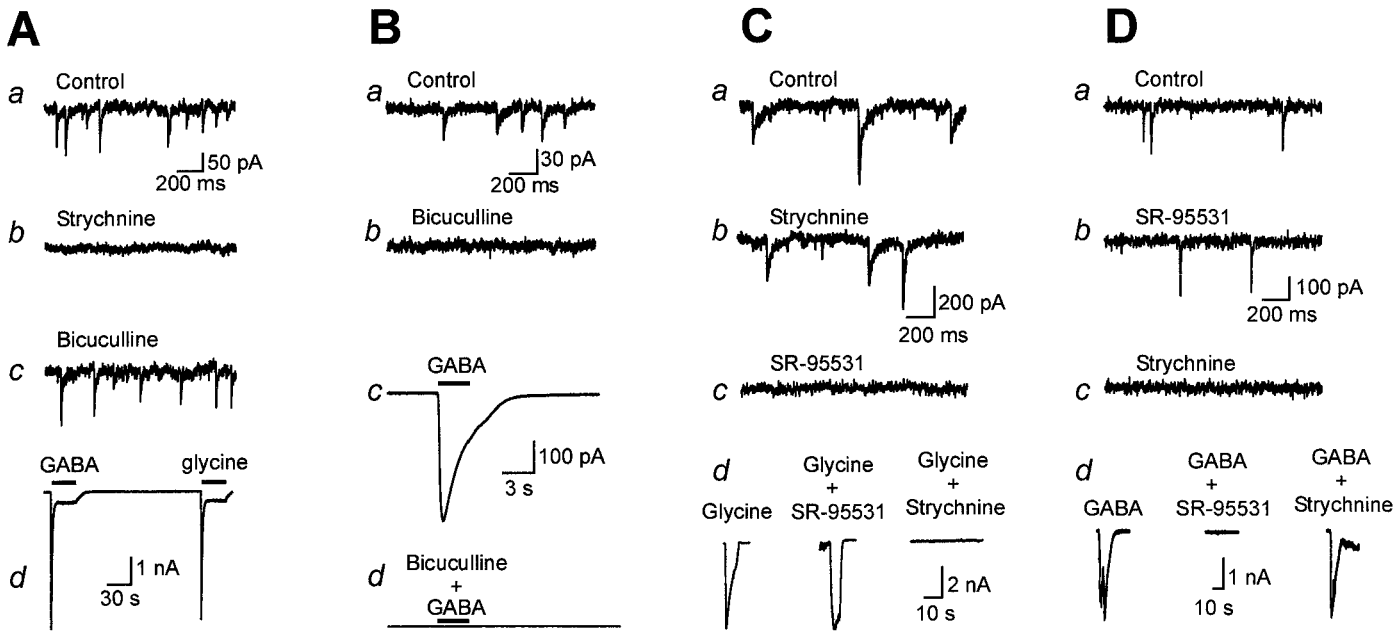

Figure 5. All laminae I-II neurons respond to exogenous application of both GABA and glycine. *A*, A lamina I neuron displaying only GlyR-mediated mIPSCs (*Aa*) because they were all selectively blocked by 100 nM strychnine (*Ab*; recovery in 10 μM bicuculline; *Ac*). Yet application of both GABA (1 mM) and glycine (1 mM) induced an inward current in this cell (*Ad*). Each of the agonists was applied by pressure ejection for 30 sec, using a micropipette positioned near the recorded cell. The holding potential is −65 mV. *B*, Both GABA-induced response and $GABA_A$R-mediated mIPSCs are blocked by bicuculline. *a*, The traces illustrate spontaneous mIPSCs recorded from a lamina II neuron. *b*, Bath-application of 10 μM bicuculline blocked all the $GABA_A$R-mediated mIPSCs. *c*, Puff-application of 1 mM GABA for 3 sec induced an inward current in this cell. *d*, The response to 1 mM GABA was blocked by 10 μM bicuculline. *C*, In this lamina II cell, the $GABA_A$R-mediated mIPSCs (*a*) are not affected by bath application of 1 μM strychnine (*b*), but selectively blocked by 3 μM SR-95531 (*c*); in the same cell, bath-applied 1 mM glycine induced an inward current, which is not affected by 3 μM SR-95531, but abolished by 1 μM strychnine (*d*). *D*, GlyR-mediated mIPSCs (*a*) in this lamina I neuron are not affected by bath-applied 3 μM SR 95531 (*b*), but selectively blocked by 100 nM strychnine (*c*); in this lamina I neuron, bath-applied 1 mM GABA induced an inward current, which was abolished by 3 μM SR-95531, but not affected by 1 μM strychnine (*d*).

taneous action potential-independent IPSCs and thus compare the results with those from the control conditions. A 25-fold increase in frequency of mIPSCs was observed on average (range, 17- to 33-fold increase). In all cases, the mIPSCs were blocked either exclusively by bicuculline (or SR-95531) or by strychnine (Fig. 6).

Large evoked IPSCs in lamina I

The observation that lamina I neurons displayed only GlyR-mediated mIPSCs, yet appeared to express both GlyRs and $GABA_A$Rs, together with the finding that virtually all glycine-immunoreactive interneurons in the superficial dorsal horn also express GABA (Todd and Sullivan, 1990), suggests that $GABA_A$Rs may not be located at synaptic junctions in lamina I neurons. By recruiting more synaptic input synchronously, accumulation of transmitter may lead to sufficient spillover from synapses to activate distant receptors (Isaacson et al., 1993). To test this possibility, we recorded monosynaptic evoked IPSCs in lamina I by placing a bipolar tungsten electrode within 20–50 μm of the recorded neurons. Large intensity stimulation (200–500 μA; 200–300 μsec duration) were used at a frequency of ≤0.3 Hz. The evoked IPSCs (eIPSCs) were only partially attenuated by 1–2 μM strychnine; the remaining component was blocked by 20 μM bicuculline ($n = 5$; Fig. 7*A*). Thus, in lamina I, there was a $GABA_A$R-mediated component of large eIPSCs. The rise time of the $GABA_A$R-mediated component of these eIPSCs was significantly slower than that of the GlyR-mediated component (6.2 ± 0.5 msec vs 2.8 ± 0.6 msec, respectively; $p < 0.005$, Fig. 7*A*). The decay time course of the GlyR-mediated component (17.1 ± 3.2 msec), was also significantly faster than that of the $GABA_A$R component (80.4 ± 30.3 msec; $p < 0.05$).

Minimal versus large evoked IPSCs in lamina I

To investigate whether the differences in rise times of the evoked GlyR- and $GABA_A$R-mediated IPSCs could reflect a difference in the location of their respective receptors, we used minimal stimuli (producing all-or-none IPSCs), using patch micropipettes placed either close to the soma (within 20–50 μm) or close to a dendrite at a distance from the cell body (150–300 μm). Because most of the neurons in lamina I have a bipolar morphology in the parasagittal plane (Light et al., 1979; Woolf and Fitzgerald, 1983; Lima and Coimbra, 1986; Ma et al., 1996), the positioning of the stimulating electrode could be achieved to reach specifically one portion of the dendrite of the recorded neuron (Fig. 8, *diagram*). In all cases tested, minimally evoked IPSCs (meIPSCs) obtained from stimulations within 20 μm from the cell body were completely blocked by 1 μM strychnine ($n = 12$; Figs. 7*B*, 8). After complete block by strychnine and after a 5- to 10-fold increase in the stimulus intensity, a slower IPSC could be evoked that was blocked by 10–20 μM bicuculline (Figs. 7*B*, 8). The rise time of the $GABA_A$R-mediated IPSCs was 2.2 ± 1.2 msec, significantly slower that that of GlyR-mediated meIPSCs (0.9 ± 0.5 msec; Fig. 7*B, inset*).

The $GABA_A$R-evoked IPSCs may have had slower rise times because they systematically originated at a more distant site from the soma than the GlyR-evoked IPSCs. For this to be the case, the $GABA_A$R evoked IPSCs resulting from stimulation proximal to the soma would have to have a significantly longer latency than

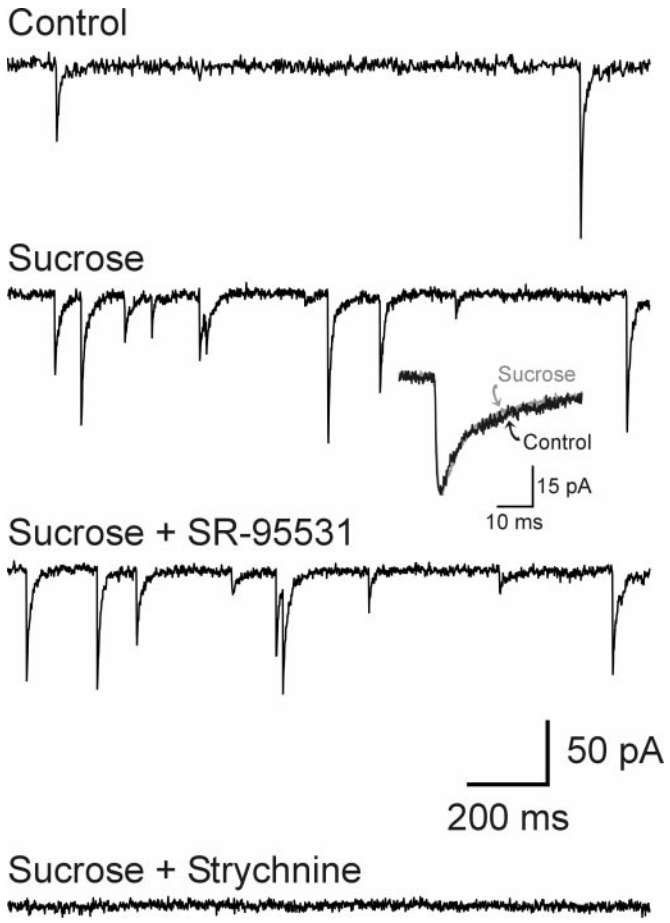

Figure 6. Hypertonic solution-induced increase in vesicular release failed to reveal a heterogeneous population of mIPSCs in laminae I-II. Pressure-application of hyperosmotic (610 mOsm) ACSF (*middle traces*) induced a 33-fold increase in the frequency of mIPSCs in this lamina I neuron. The mIPSCs were not affected by bath-application of 3 μM SR-95531, but selectively blocked by 100 nM strychnine. The superimposed averages in the *inset* show the lack of change in mIPSC kinetics in sucrose to further confirm that no new class of mIPSC was revealed by the hyperosmotic solution.

GlyR-evoked IPSCs (i.e., proximal stimuli producing $GABA_A$R IPSCs would have to activate fibers that travel a longer distance to reach distal portions of the postsynaptic cell). We thus compared the latencies of the different components with each type of stimuli.

The latency of both GlyR and $GABA_A$R-mediated components was comparable (1.2 ± 0.2 vs 1.7 ± 0.4 msec; $p > 0.1$). Similarly, the latency of GlyR-mediated meIPSCs elicited by stimulation close to the soma versus that in the vicinity of a distal portion of a dendrite were not significantly different (1.2 ± 0.2 vs 1.7 ± 0.6 msec, respectively). Moreover, stimulation at a >100 μm distance from the soma but also away from the vicinity of a dendrite always failed to produce IPSCs. Evoked $GABA_A$R-mediated IPSCs (using larger stimulus intensities) at these same proximal and distal sites of stimulation had also comparable latencies (1.7 ± 0.4 vs 2.1 ± 0.9 msec, respectively). Finally, a comparison of the rise time of GlyR-mediated meIPSCs originating at a site proximal or distal to the soma revealed little prolongation (0.7 ± 0.6 vs 0.9 ± 0.5 msec, respectively; Fig. 8*A*), consistent with the short membrane time constant of these cells (15.2 ± 6.8 msec; range, 2.5–45.3 msec). Proximal and distal $GABA_A$R-mediated IPSCs also had comparable rise times (2.2 ± 1.2 vs 2.3 ± 1.1 msec, respectively; Fig. 8*B*). The decay time constant of the GlyR and $GABA_A$R components evoked by these focal stimulations were 10.8 ± 1.7 msec versus 42.7 ± 6.0 msec, respectively.

Thus, it appeared that both $GABA_A$R- and GlyR-mediated IPSCs could originate at similar electrotonic distance from the soma. Eliciting $GABA_A$R-mediated IPSCs, however, always required stronger stimulus intensities that produced synaptic events with significantly slower rising and decaying kinetics than their GlyR-mediated counterpart. Taken together, these results indicated that the slower rising phase of evoked $GABA_A$R-mediated IPSCs appeared not to be caused by a more distant site of origin but rather a slower, likely diffuse or distant activation of $GABA_A$R after sufficient accumulation of released GABA.

Effect of flunitrazepam on miniature IPSCs in lamina I

The results from mIPSCs and stimulus-evoked IPSCs suggested that either different threshold for glycine and GABA release or subthreshold activation of $GABA_A$Rs by single vesicles of GABA. To distinguish between these two possibilities, we aimed at raising the sensitivity of $GABA_A$Rs with the benzodiazepine flunitrazepam, to potentiate possible subliminal responses to GABA released by single vesicles of transmitter. In the presence of 1 μM flunitrazepam, the rise time of mIPSCs was significantly prolonged to 2.4 ± 0.3 msec, and the decay time constant increased to 27 ± 4.2 msec (vs 0.6 ± 0.1 and 6.0 ± 0.3 msec in control; $n = 7$; Fig. 9). Close examination of the distribution of rise times and decay time constants (Fig. 9*B–D*) indicates that the large majority of mIPSCs had their kinetics prolonged by flunitrazepam. Addition of 100 nM strychnine to the bath solution containing flunitrazepam revealed mIPSCs with very slow rise time (4.1 ± 0.9 msec); 10 times more prolonged than that of GlyR mIPSCs in lamina I neurons and of $GABA_A$R mIPSCs in neurons of deeper laminae. Similarly, the decay kinetics (52.8 ± 8.9 msec) were ~10× slower than that of the GlyR mIPSCs in lamina I neurons and 5× slower that of $GABA_A$R mIPSCs in lamina II. Addition of 10 μM bicuculline completely abolished all of these remaining slow mIPSCs, indicating that they were $GABA_A$R-mediated. The frequency of mIPSCs in flunitrazepam was slightly increased (20–30%) over that in control conditions, most likely because, at some junctions, no synaptic glycine receptors were present. Importantly however, the frequency of the very slow $GABA_A$R mIPSCs that persisted in the presence of strychnine and flunitrazepam was always >75% of that of the number of events in control conditions and more than twice the increase in frequency observed in the presence of flunitrazepam alone (Fig. 9*B,C*). There was also <11% overlap in areas between the distributions of decay time constants in control versus flunitrazepam (Fig. 9*D*). This therefore indicated that the majority of individual mIPSCs had a dual GlyR and $GABA_A$R component. Given the fact that mIPSCs are likely reflecting responses to single vesicles of transmitter, these results indicate co-storage of GABA and glycine in the same synaptic vesicles.

Effects of GABA uptake inhibitors on IPSCs in lamina I

Because GABA uptake inhibitors do not affect the amplitude or the time course of mIPSCs, it is thought that clearance of GABA from the synaptic cleft is not a limiting factor determining the decay time course of mIPSCs (Thompson and Gahwiler, 1992; Isaacson et al., 1993). On the other hand, the uptake blockers prolong large evoked $GABA_A$R-mediated IPSCs. If the GABA

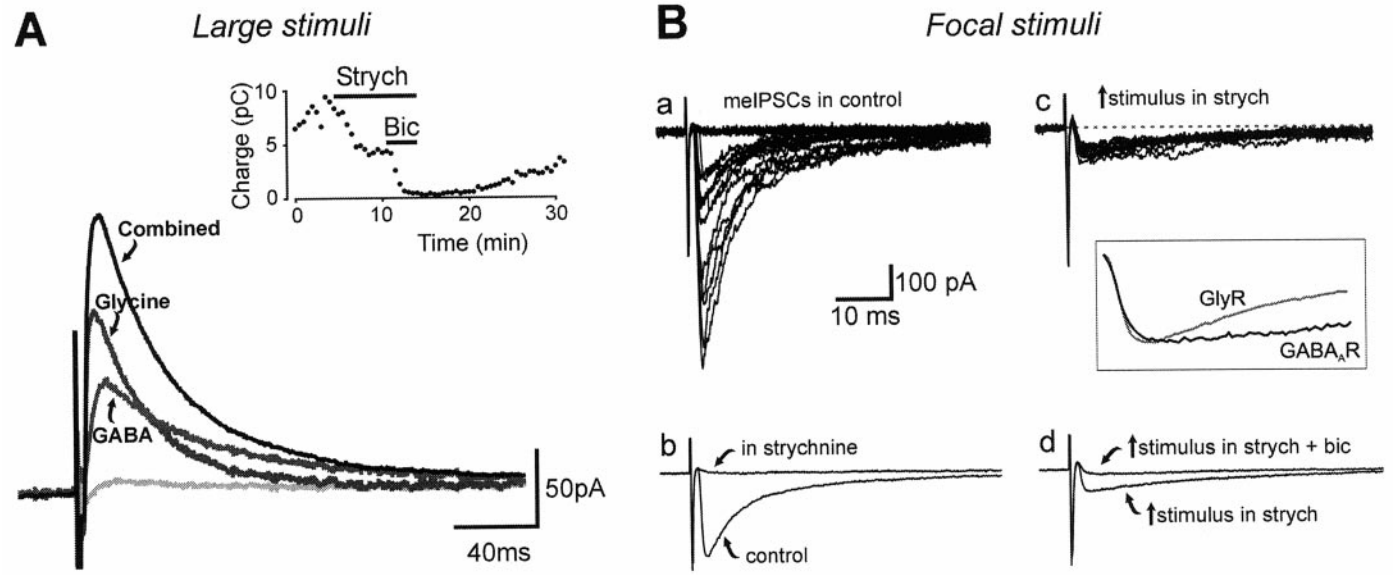

Figure 7. Large stimulus-evoked IPSCs in lamina I reveal a $GABA_A$R-mediated component. *A*, Average of 48 IPSCs elicited by placing a tungsten electrode within 300 μm from the cell body of the recorded neuron (*Combined*). The membrane potential was held at +40 mV to avoid activation of voltage-sensitive Na^+ currents. After the application of 2 μM strychnine, a component remained (*GABA*) that could be blocked by 20 μM bicuculline. The GlyR-mediated component (*Glycine*) was obtained by subtraction of the *GABA* trace from the *Combined* trace. The *inset* shows the time course of block of evoked $GABA_A$R- and GlyR-mediated IPSCs (quantified by the area under the curve, i.e., charge). *Ba,* Superimposed minimally evoked IPSCs (meIPSCs) obtained by focal stimuli applied within 20 μm from the cell body using a patch micropipette. These meIPSCs were completely blocked by 1–2 μM strychnine (*b*, average of 25 traces). *c*, A sixfold increase in stimulus intensity elicited $GABA_A$R-mediated IPSCs that could be blocked by addition of 10–20 μM bicuculline (*d*, average of 15 traces). The *inset* illustrates the $GABA_A$R- and GlyR-mediated components scaled to the same amplitude; note the slower rising and decay phases of the $GABA_A$R component.

released by single vesicles at lamina I synapse is insufficient to activate distant $GABA_A$Rs, blocking uptake should not significantly affect mIPSCs. On the other hand, with "spillover" of GABA from several neighboring synapses activated synchronously, blocking uptake may favor temporal summation of extracellular GABA originating from adjacent sources (Isaacson et al., 1993). We first tested the effects of tiagabine (25–50 μM) and NO-711 (10–30 μM) of normal mIPSCs in lamina I ($n = 7$). Neither uptake blocker had a detectable effect on these mIPSCs (Fig. 10). After tiagabine or NO-711 administration, eIPSCs had significantly reduced peak amplitude, and their decay time courses were prolonged ($n = 5$; mean increase in decay of the late component of 44 ± 3 msec; $p < 0.01$; Fig. 10).

Uptake may be important in limiting the extent of extrasynaptic receptor activation (Isaacson et al., 1993; Asztely et al., 1997). Yet, failure to detect an effect of the uptake inhibitor on miniature events may simply reflect that the amount of "spillover" during a miniature event is subliminal for activation of these receptors. At glutamate synapses for example, spillover of transmitter after release of a single vesicle appears to be relevant only for NMDA receptors because they have a much higher affinity for the transmitter than AMPA receptors. It may be expected, therefore, that raising the affinity of extrasynaptic $GABA_A$ receptors with a benzodiazepine could reveal a significant effect of the uptake blocker on mIPSCs. To test this, we recorded pure $GABA_A$R mIPSCs in lamina I revealed in the presence of 1 μM flunitrazepam and 100 nM strychnine to test for the effect of the uptake inhibitors. Tiagabine and NO-711 administration decreased the frequency of mIPSCs and significantly prolonged their decay time course (from 62.3 ± 8.7 to 106.7 ± 10.2 msec; $p < 0.05$; $n = 5$; Fig. 10). In all cases, subsequent addition of 10 μM bicuculline or 3 μM SR-95531 abolished all of these mIPSCs.

DISCUSSION

Our results indicate that GABA and glycine mediate separate miniature IPSCs with distinct kinetics in superficial dorsal horn neurons of the rat spinal cord, and these cells are usually bombarded by one type of mIPSC only. Even in cells with both types of mIPSCs present, these synaptic events represent separate populations. The differences in kinetics of the GlyR- versus $GABA_A$R-mediated mIPSCs are consistent with previous findings in the dorsal horn (Takahashi and Momiyama, 1991; Takahashi et al., 1992; Baba et al., 1994; Yoshimura and Nishi, 1993, 1995) and in medullary neurons (Lewis and Faber, 1996; Grudt and Henderson, 1998), in contrast with retinal ganglion cells in which $GABA_A$R-mediated IPSCs have a faster decay than GlyR-mediated ones (Protti et al., 1997).

Immunocytochemical studies by Todd and Sullivan (1990) demonstrated that the proportion of glycine-immunoreactive neurons in laminae I, II, and III were 9, 14, and 30%, respectively. The proportions of GABA-immunoreactive neurons in laminae I, II, and III were higher: 28, 31, and 46%, respectively. They also reported that virtually all of the glycine-immunoreactive cells in this area were also GABA-immunoreactive, but many GABA-immunoreactive cells do not show immunoreactivity to glycine. Thus, while recording from laminae I-II, one would expect that the neurons displaying GlyR-mediated mIPSCs would also show $GABA_A$R-mediated mIPSCs. On the contrary, we found namely that lamina I neurons were bombarded exclusively by GlyR-mediated mIPSCs in normal conditions. Thus, glycine appears to

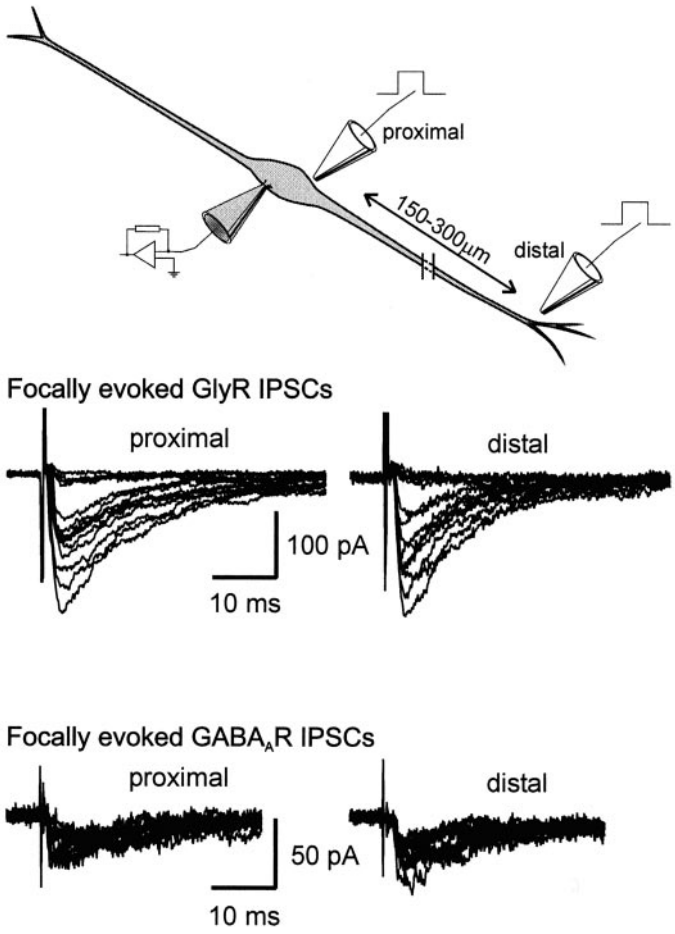

Figure 8. Comparable latencies, rise times, and amplitudes of proximal and distal $GABA_A$R- and GlyR-mediated meIPSCs. The diagram at the *top* illustrates how the micropipettes were positioned for focal stimulation along the bipolar axis of lamina I neurons. Focal stimuli were applied within 20 μm from the cell body (*proximal*), and within 20–70 μm of a distal dendrite located at 150–300 μm distance from the soma (*distal*). *Top traces*, Superimposed GlyR-mediated meIPSCs elicited in the presence of 10 μM bicuculline. *Bottom traces*, In the presence of 1 μM strychnine, $GABA_A$R-mediated IPSCs with slower kinetics could be evoked. Note the slightly longer latencies for both the distal $GABA_A$R- and GlyR-mediated evoked IPSCs, but the very similar rise times and amplitudes. The only slight increase in latency of the distally evoked IPSCs account for an approximately twofold conduction distance and thus indicated that these IPSCs still originated at a significant distance from the soma. In any case, the distally evoked $GABA_A$R-mediated events did not have a shorter latency then their GlyR counterparts, arguing against the possibility that $GABA_A$R IPSCs are only occurring at distal points from the soma. Moreover, the only slight slowing of the rising phase of the distal GlyR-mediated meIPSCs indicate little space clamp limitations in these cells and thus ruling out the possibility that $GABA_A$R-mediated mIPSCs may exist that could not be detected by somatic recording.

be solely responsible for tonic inhibition of second order neurons in this layer.

Co-release of glycine and GABA from the same vesicle

Unmasking of a very slow rising and decaying $GABA_A$ component of mIPSCs in lamina I with flunitrazepam provided an ideal tool to address the issue of co-storage of GABA and glycine in the same vesicles. Importantly, the whole distribution of rise times and decay time constants was shifted in the presence of the benzodiazepine with little overlap with the control distribution, indicating that the majority of the events were affected. Accordingly, the increase in frequency of events observed in the presence of the benzodiazepine was much lower than the number of $GABA_A$R-mediated mIPSCs remaining in the presence of strychnine. Thus, it can be concluded that the majority of mIPSCs had a dual GlyR- and $GABA_A$R-mediated component. Because mIPSCs appear to reflect postsynaptic responses to the release of single vesicles of transmitter, the data strongly indicated the co-storage of glycine and GABA in the same vesicles. This is consistent with similar recent evidence at the immature motoneuron synapse (Jonas et al., 1998) as well as with the observation that both transmitters can be carried by the same vesicular transporter (Christensen and Fonnum, 1991; Burger et al., 1991) present at both glycinergic and GABAergic synapses (Chaudhry et al., 1998; Dumoulin et al., 1999). Whereas the evidence presented by Jonas et al. (1998) relied on template fits of the decay phase of mIPSCs, our evidence has the added advantage that the rising kinetics of the $GABA_A$ component was also dramatically slower than that of the GlyR component and that the events were sufficiently altered after the benzodiazepine administration that it was possible to quantify the degree of overlap between the distributions of events for each kinetic parameter, providing an even more compelling argument for the co-storage of GABA and glycine.

Extrajunctional $GABA_A$R activation in lamina I

Several pieces of evidence converge to indicate that, in contrast to GlyRs, $GABA_A$Rs are likely located extrasynaptically in lamina I: (1) the absence of $GABA_A$R-mediated spontaneous and miniature IPSCs while the cells received GlyR-mediated mIPSC and all responded to exogenous application of GABA in a bicuculline-dependent matter; (2) activation of several inhibitory synapses synchronously (large evoked IPSCs) revealed a $GABA_A$ component; (3) the evoked $GABA_A$R component had a similar latency, yet slower rising kinetics than the GlyR component; (4) benzodiazepines can unmask a $GABA_A$ component to individual mIPSCs, and this component has extremely slow rising kinetics (10× slower than GlyR mIPSCs in lamina I or $GABA_A$R mIPSCs in deeper laminae); (5) specific blockers of GABA uptake did not affect normal mIPSCs in lamina I but significantly prolonged the decay kinetics of evoked IPSCs that involve synchronous activation of neighboring synapses as well as of $GABA_A$R mIPSCs unmasked by flunitrazepam (in the presence of strychnine).

The slow kinetics of $GABA_A$R-mediated IPSCs in lamina I could suggest that they specifically originate at distant sites from the soma [therefore subject to greater space clamp attenuation (Spruston et al., 1994)]. However, the short time constant of lamina I neurons and the lack of difference in the kinetics of proximally versus distally evoked IPSCs argues against this possibility. More importantly, the dual-component mIPSCs in flunitrazepam clearly show that the slow $GABA_A$ components originated from the same release sites as the fast-rising GlyR components.

Extrasynaptic distribution of $GABA_A$ receptor subunits have often been described in the spinal cord and other brain regions (Somogyi et al., 1989; Soltesz et al., 1990; Bohlhalter et al., 1994; Nusser et al., 1998). In the dorsal horn, β_2/β_3 subunit immunoreactivity, possibly the most widely expressed subunits in the spinal cord, appeared often extrasynaptically (Alvarez et al., 1996). It may be however difficult to draw definitive conclusions from studies on the subcellular distribution of $GABA_A$Rs with pre-

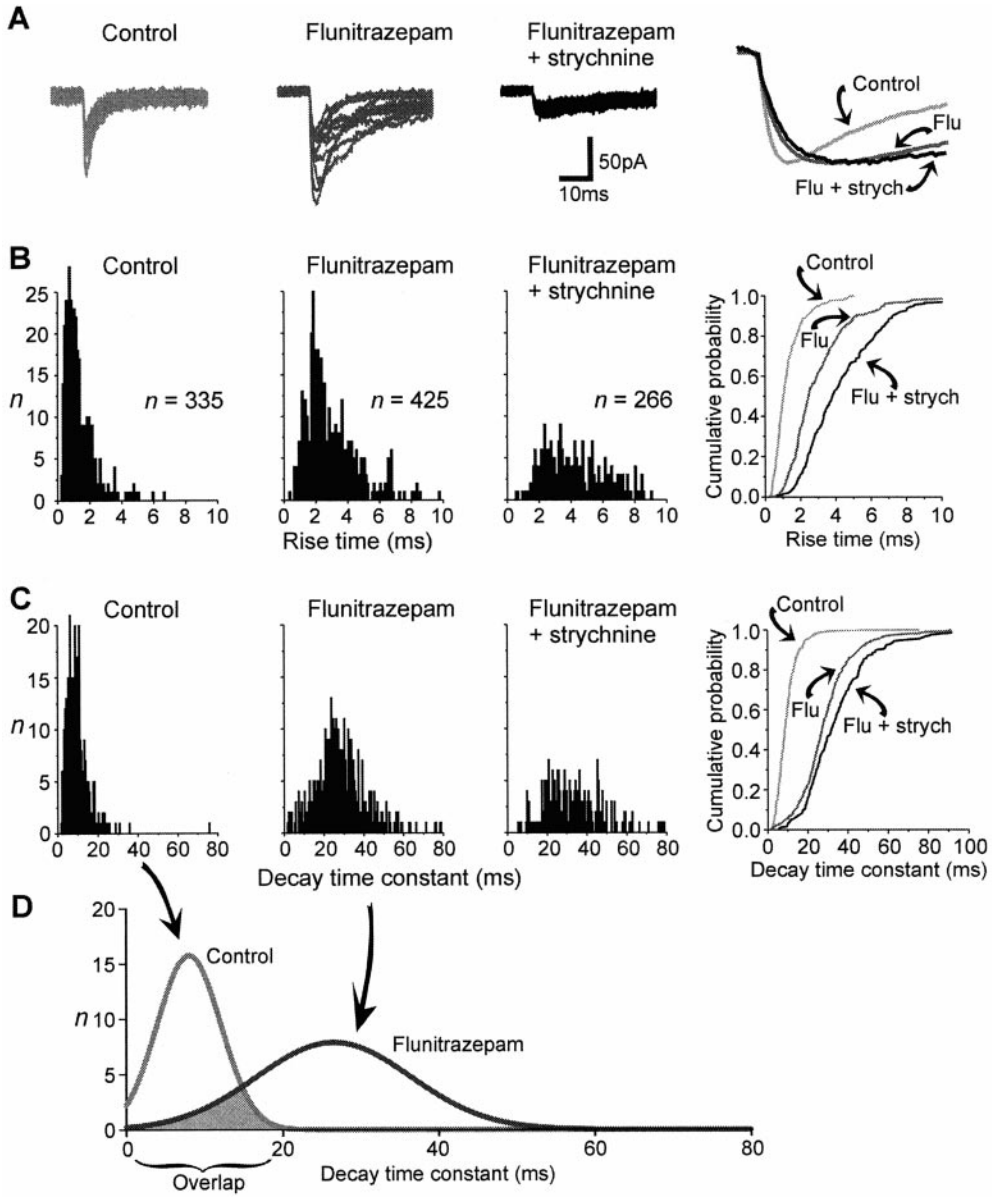

Figure 9. The benzodiazepine flunitrazepam unmasks a slow $GABA_A$R-mediated component to mIPSC recorded in lamina I neurons. The traces in *A* are representative superimposed mIPSCs used to compile the histograms below each trace (*B*, *C*). The *inset* at the *right top corner* is a superimposition of the events scaled to the same amplitude to emphasize their difference in rising and decaying kinetics. The histograms in *B* and *C* illustrate the distributions of 10–90% rise times and decay time constants for all the events detected in each condition during a 7 min window. Thus, the number of events in each histogram provides an estimate of the frequency of events in each condition. The curve in *D* illustrates the area overlap between the Gaussian curves fit to the histograms above. The overlap (*gray area*) was <11% of the area under the curve for the control histogram. The very small overlap between the distributions or rise times and decay time constants between control conditions and in the presence of flunitrazepam indicates that the majority of individual mIPSCs had their kinetics altered. Consistent with this observation, the number of events remaining in the presence of flunitrazepam and strychnine is greater than the difference between the number of events detected in flunitrazepam versus control. Addition of 10 μM bicuculline completely abolished all mIPSCs that remained in the presence of 100 nM strychnine. The graphs on the *right* are cumulative histograms illustrating the intermediate distribution of kinetics observed between control, flunitrazepam (*Flu*), and flunitrazepam plus 100 nM strychnine (*Flu + strych*) conditions.

embedding approaches because of the limited access of some antigenic sites (Nusser et al., 1995). Nevertheless, even with pre-embedding approaches, antibodies directed against an intracellular loop of the receptor may have better access to postsynaptic densities (active zones) (Todd et al., 1996). Interestingly, whereas Todd et al. (1996) found punctate staining for the β_3 subunit in deeper laminae, the labeling often extended beyond active sites in laminae I-II. In fact, it was often difficult to localize precisely the β_3 staining in these laminae (A. J. Todd, personal communication). For this reason, they refrained from further quantifying β_3 versus gephyrin immunoreactivity in lamina I. Thus, although immunocytochemical evidence may be consistent with the possibility of a prominent extrasynaptic distribution of $GABA_A$Rs in lamina I, no direct data are available.

Evidence with benzodiazepines rules out the possibility of a specifically higher threshold for activation of interneurons releasing GABA. The very slow rise time of $GABA_A$R-mediated mIPSCs revealed by flunitrazepam suggests that either very little GABA is contained in glycine-containing synaptic vesicles or that the $GABA_A$Rs are located at a distance from the site of release. No evidence is available, however, to indicate that a very low level of GABA in synaptic vesicles may occur. In fact, all available evidence suggest the opposite (Mody et al., 1994). Furthermore, this possibility would appear highly unlikely in the present case, because the vesicular transporter has a greater affinity for GABA than glycine (Burger et al., 1991; Christensen and Fonnum, 1991) and because substantial levels of immunoreactivity for GABA is detected in these cells (Todd and Sullivan, 1990) and their terminals (Todd et al., 1996). Finally, whereas results from rapid applications of GABA to excised membrane patches would tend to link slow rise times with low agonist concentration (Maconochie et al., 1994), it is interesting to note that with very brief transients of transmitter [as seems to be the case in the cleft (Destexhe and Sejnowski, 1995; Clements, 1996)], even very low concentrations of GABA generate currents with fast rise times (Galarreta and Hestrin, 1997). Low concentration of GABA is also not expected to generate longer decay time courses (Maconochie et al., 1994; Galarreta and Hestrin, 1997) that could not

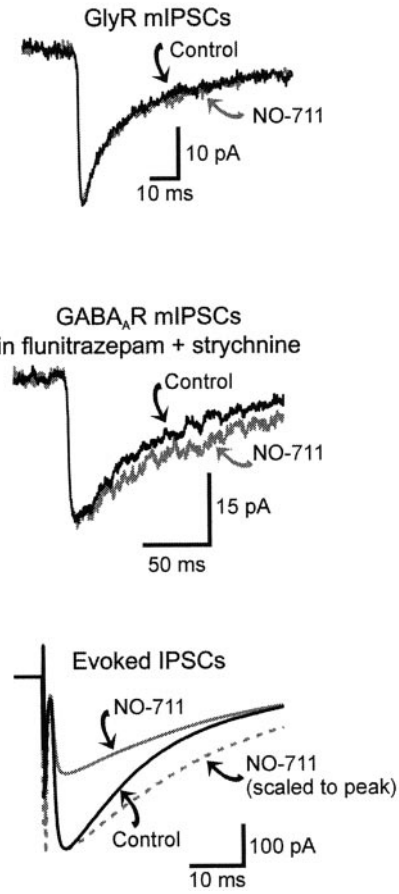

Figure 10. GABA uptake blockers do not significantly affect GlyR-mediated mIPSCs in lamina I but prolong the decay time course of evoked IPSCs and of $GABA_A$R-mediated mIPSCs revealed by flunitrazepam. The traces at the *top* are averages of 89 consecutive mIPSCs in control solution and 100 mIPSCs after 30 min of bathing in 30 μM NO-711. The traces in the *middle* are averages of 23 mIPSCs recorded in the presence of 1 μM flunitrazepam and 100 nM strychnine before and after addition of 30 μM NO-711 (scaled averages). The traces at the *bottom* are averages of 42 stimulus-evoked IPSCs in control solution and 57 evoked IPSCs after 20 min of bathing in 10 μM NO-711 (10 M QX-314 was added to the pipette solution to block voltage-sensitive Na channels).

account for the much slower decay of the $GABA_A$R components in lamina I versus those recorded in lamina II [see also discussion in (Rossi and Hamann, 1998)]. Thus, the most plausible explanation for our results is that $GABA_A$Rs are located at a distance from the vesicle release site, suggesting a prominent perisynaptic distribution of functional $GABA_A$Rs at these synapses (Fig. 11).

Functional significance of the difference in $GABA_A$R- and GlyR-mediated inhibition in lamina I

Symptoms very similar to those observed in neuropathic pain models involving peripheral nerve constriction can also be obtained with intrathecal administration of subconvulsant doses of strychnine or bicuculline (Yaksh, 1989; Sivilotti and Woolf, 1994). Importantly, strychnine-induced hypersensitivity is selective to non-noxious input (allodynia) and is morphine-insensitive (Sherman and Loomis, 1994, 1995, 1996; Sorkin and Puig, 1996). Moreover, the sensitization produced does not only affect spinal segmental nociceptive reflexes, but also ascending nociceptive pathways (Sherman et al., 1997a,b). Thus $GABA_A$ and glycine receptor-mediated inhibition appear to play an important role in

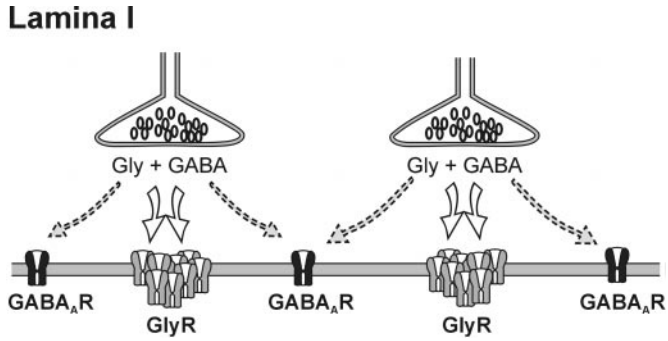

Figure 11. Proposed summary of glycine versus $GABA_A$ receptor-mediated inhibition in lamina I. During normal basal activity, both glycine and GABA may be released, but only glycine receptors that are clustered at synapses will mediate the mIPSCs, whereas extrasynaptic $GABA_A$Rs may require accumulation of GABA "spillover". Thus, in lamina I, glycine appears to mediate tonic inhibition from spontaneous vesicular release. In contrast, $GABA_A$R-mediated inhibition may be effective to control larger, synchronous (evoked) input.

the regulation of excitability in specific nociceptive sensory pathways in the dorsal horn, and blockade of this control appears to unveil subliminal innocuous input to neurons in these pathways.

The present finding of the differential distribution of $GABA_A$ and glycine receptor-mediated mIPSCs among cell types and especially the finding that only glycine is responsible for the tonic inhibition of lamina I neurons suggests separate roles for these two inhibitory systems. The selective tonic inhibition exerted by glycine on lamina I neurons may be contrasted to evoked inhibition mediated by GABA acting on $GABA_A$ receptors. Blockade of either type of control may differentially affect nociceptive integration. For example, the difference in kinetics of the GABAergic versus glycinergic IPSCs and the type of activity that recruit them may match the nature of excitatory input they control. Interestingly, metabotropic receptor antagonists attenuate bicuculline-induced allodynia but are not effective against strychnine-induced allodynia (Onaka et al., 1996). Metabotropic glutamate receptors appear to be mainly located at extrasynaptic sites (Baude et al., 1993) and may therefore be activated selectively after release of a sufficient concentration of glutamate that can spill over the synapses (Rusakov and Kullmann, 1998). This property may match that guiding activation of $GABA_A$Rs in lamina I (also because of their perisynaptic distribution). Thus, subcellular segregation of $GABA_A$Rs and GlyRs confers distinct functional roles to inhibition mediated by these two transmitters in lamina I.

REFERENCES

Alvarez FJ, Taylor-Blake B, Fyffe RE, De BA, Light AR (1996) Distribution of immunoreactivity for the β_2 and β_3 subunits of the $GABA_A$ receptor in the mammalian spinal cord. J Comp Neurol 365:392–412.

Asztely F, Erdemli G, Kullmann DM (1997) Extrasynaptic glutamate spillover in the hippocampus: dependence on temperature and the role of active glutamate uptake. Neuron 18:281–293.

Baba H, Yoshimura M, Nishi S, Shimoji K (1994) Synaptic responses of substantia gelatinosa neurones to dorsal column stimulation in rat spinal cord *in vitro*. J Physiol (Lond) 478:87–99.

Baude A, Nusser Z, Roberts JDB, Mulvihill E, McIlhinney RAJ, Somogyi P (1993) The metabotropic glutamate receptor (mGluR1a) is concentrated at perisynaptic membrane of neuronal subpopulations as detected by immunogold reaction. Neuron 11:771–787.

Bohlhalter S, Mohler H, Fritschy JM (1994) Inhibitory neurotransmission in rat spinal cord: co-localization of glycine- and $GABA_A$-receptors at GABAergic synaptic contacts demonstrated by triple immunofluorescence staining. Brain Res 642:59–69.

Bohlhalter S, Weinmann O, Mohler H, Fritschy JM (1996) Laminar compartmentalization of $GABA_A$-receptor subtypes in the spinal cord: an immunohistochemical study. J Neurosci 16:283–297.

Burger PM, Hell J, Mehl E, Krasel C, Lottspeich F, Jahn R (1991) GABA and glycine in synaptic vesicles: storage and transport characteristics. Neuron 7:287–293.

Chéry N, De Koninck Y (1997) GABA and glycine mediate separate miniature IPSCs in identified laminae I-II neurons of the adult rat spinal dorsal horn. Soc Neurosci Abstr 23:2341.

Chéry N, De Koninck Y (1998) Synaptic *vs*. non-synaptic glycine and $GABA_A$ receptors in identified lamina I neurons of the adult rat spinal dorsal horn. Soc Neurosci Abstr 24:390.

Chaudhry FA, Reimer RJ, Bellocchio EE, Danbolt NC, Osen KK, Edwards RH, Storm-Mathisen J (1998) The vesicular GABA transporter, VGAT, localizes to synaptic vesicles in sets of glycinergic as well as GABAergic neurons. J Neurosci 18:9733–9750.

Chen QX, Stelzer A, Kay AR, Wong RK (1990) $GABA_A$ receptor function is regulated by phosphorylation in acutely dissociated guinea-pig hippocampal neurones. J Physiol (Lond) 420:207–221.

Christensen H, Fonnum F (1991) Uptake of glycine, GABA and glutamate by synaptic vesicles isolated from different regions of rat CNS. Neurosci Lett 129:217–220.

Clements JD (1996) Transmitter timecourse in the synaptic cleft: its role in central synaptic function. Trends Neurosci 19:163–171.

Craig AD (1994) Spinal and supraspinal processing of specific pain and temperature. In: Touch, temperature, and pain in health and disease. Progress in Brain Research and Management, Vol 3 (Boivie J, Hansson P, Lindblom U, eds), pp 421–437. Seattle: IASP.

Craig AD (1996) Pain, temperature, and the sense of the body. In: Somesthesis and the neurobiology of the somatosensory cortex (Franzen O, Johansson RS, Terenius L, eds), pp 27–39. Basel: Birkhauser.

De Koninck Y, Chéry N (1998) Visual identification of lamina I and morphological classification of its neurons in live adult rat spinal cord slices. Soc Neurosci Abstr 24:390.

De Koninck Y, Mody I (1994) Noise analysis of miniature IPSCs in adult rat brain slices; properties and modulation of synaptic $GABA_A$ receptor channels. J Neurophysiol 71:1318–1335.

De Koninck Y, Mody I (1996) The effects of raising intracellular calcium on synaptic $GABA_A$ receptor-channels. Neuropharmacology 35:1365–1374.

De Koninck Y, Ribeiro-da-Silva A, Henry JL, Cuello AC (1992) Spinal neurons exhibiting a specific nociceptive response receive abundant substance P-containing synaptic contacts. Proc Natl Acad Sci USA 89:5073–5077.

Destexhe A, Sejnowski TJ (1995) G protein activation kinetics and spillover of gamma-aminobutyric acid may account for differences between inhibitory responses in the hippocampus and thalamus. Proc Natl Acad Sci USA 92:9515–9519.

Dumoulin A, Rostaing P, Bedet C, Levi S, Isambert MF, Henry JP, Triller A, Gasnier B (1999) Presence of the vesicular inhibitory amino acid transporter in GABAergic and glycinergic synaptic terminal boutons. J Cell Sci 112:811–823.

Galarreta M, Hestrin S (1997) Properties of $GABA_A$ receptors underlying inhibitory synaptic currents in neocortical pyramidal neurons. J Neurosci 17:7220–7227.

Grudt TJ, Henderson G (1998) Glycine and $GABA_A$ receptor-mediated synaptic transmission in rat substantia gelatinosa: inhibition by μ-opioid and $GABA_B$ agonists. J Physiol (Lond) 507:473–483.

Grudt TJ, Williams JT (1994) mu-Opioid agonists inhibit spinal trigeminal substantia gelatinosa neurons in guinea pig and rat. J Neurosci 14:1646–1654.

Isaacson JS, Solis JM, Nicoll RA (1993) Local and diffuse synaptic actions of GABA in the hippocampus. Neuron 10:165–175.

Jackson MB (1992) Cable analysis with the whole-cell patch clamp. Theory and experiment. Biophys J 61:756–766.

Jonas P, Bischofberger J, Sandkuhler J (1998) Corelease of two fast neurotransmitters at a central synapse. Science 281:419–424.

Lewis CA, Faber DS (1996) Properties of spontaneous inhibitory synaptic currents in cultured rat spinal cord and medullary neurons. J Neurophysiol 76:448–460.

Light AR (1992) The initial processing of pain and its descending control: spinal and trigeminal systems. Basel: Karger.

Light AR, Trevino DL, Perl ER (1979) Morphological features of functionally defined neurons in the marginal zone and substantia gelatinosa of the spinal dorsal horn. J Comp Neurol 186:151–171.

Lima D, Coimbra A (1986) A Golgi study of the neuronal population of the marginal zone (lamina I) of the rat spinal cord. J Comp Neurol 244:53–71.

Ma W, Ribeiro-da-Silva A, De Koninck Y, Radhakrishnan V, Henry JL, Cuello AC (1996) Quantitative analysis of substance P immunoreactive boutons on physiologically characterized dorsal horn neurons in the cat lumbar spinal cord. J Comp Neurol 376:45–64.

Maconochie DJ, Zempel JM, Steinbach JH (1994) How quickly can $GABA_A$ receptors open? Neuron 12:61–71.

Mitchell K, Spike RC, Todd AJ (1993) An immunocytochemical study of glycine receptor and GABA in laminae I-III of rat spinal dorsal horn. J Neurosci 13:2371–2381.

Mody I, De Koninck Y, Otis TS, Soltesz I (1994) Bridging the cleft at GABA synapses in the brain. Trends Neurosci 17:517–525.

Nusser Z, Roberts JD, Baude A, Richards JG, Somogyi P (1995) Relative densities of synaptic and extrasynaptic $GABA_A$ receptors on cerebellar granule cells as determined by a quantitative immunogold method. J Neurosci 15:2948–2960.

Nusser Z, Sieghart W, Somogyi P (1998) Segregation of different $GABA_A$ receptors to synaptic and extrasynaptic membranes of cerebellar granule cells. J Neurosci 18:1693–1703.

Onaka M, Minami T, Nishihara I, Ito S (1996) Involvement of glutamate receptors in strychnine- and bicuculline-induced allodynia in conscious mice. Anesthesiology 84:1215–1222.

Otis TS, De Koninck Y, Mody I (1994) Lasting potentiation of inhibition is associated with an increased number of $GABA_A$ receptors activated during miniature inhibitory postsynaptic currents. Proc Natl Acad Sci USA 91:7698–7702.

Perl ER (1984) Pain and nociception. In: Sensory processes (Darian-Smith I, ed), pp 915–975. Bethesda: American Physiological Society.

Protti DA, Gersshenfeld HM, Llano I (1997) GABAergic and glycinergic IPSCs in ganglion cells of rat retinal slices. J Neurosci 17:6075–6085.

Rall W (1969) Distributions of potential in cylindrical coordinates and time constants for a membrane cylinder. Biophys J 9:1509–1541.

Ribeiro-da-Silva A (1995) Substantia gelatinosa of spinal cord. In: The rat nervous system (Paxinos G, ed), pp 47–59. Sydney: Academic.

Rosenmund C, Stevens CF (1996) Definition of the readily releasable pool of vesicles at hippocampal synapses. Neuron 16:1197–1207.

Rossi DJ, Hamann M (1998) Spillover-mediated transmission at inhibitory synapses promoted by high affinity α6 subunit GABA(A) receptors and glomerular geometry. Neuron [Erratum (1998) 21:527] 20:783–795.

Rusakov DA, Kullmann DM (1998) Extrasynaptic glutamate diffusion in the hippocampus: ultrastructural constraints, uptake, and receptor activation. J Neurosci 18:3158–3170.

Sherman SE, Loomis CW (1994) Morphine insensitive allodynia is produced by intrathecal strychnine in the lightly anesthetized rat. Pain 56:17–29.

Sherman SE, Loomis CW (1995) Strychnine-dependent allodynia in the urethane-anesthetized rat is segmentally distributed and prevented by intrathecal glycine and betaine. Can J Physiol Pharmacol 73:1698–1705.

Sherman SE, Loomis CW (1996) Strychnine-sensitive modulation is selective for non-noxious somatosensory input in the spinal cord of the rat. Pain 66:321–330.

Sherman SE, Luo L, Dostrovsky JO (1997a) Spinal strychnine alters response properties of nociceptive-specific neurons in rat medial thalamus. J Neurophysiol 78:628–637.

Sherman SE, Luo L, Dostrovsky JO (1997b) Altered receptive fields and sensory modalities of rat VPL thalamic neurons during spinal strychnine-induced allodynia. J Neurophysiol 78:2296–2308.

Sivilotti L, Woolf CJ (1994) The contribution of $GABA_A$ and glycine receptors to central sensitization: disinhibition and touch-evoked allodynia in the spinal cord. J Neurophysiol 72:169–179.

Soltesz I, Roberts JDB, Takagi H, Richards JG, Mohler H, Somogyi P (1990) Synaptic and nonsynaptic localization of benzodiazepine/$GABA_A$ receptor/Cl- channel complex using monoclonal antibodies in the dorsal lateral geniculate nucleus of the cat. Eur J Neurosci 2:414–429.

Somogyi P, Takagi H, Richards JG, Mohler H (1989) Subcellular localization of benzodiazepine/$GABA_A$ receptors in the cerebellum of rat, cat, and monkey using monoclonal antibodies. J Neurosci 9:2197–2209.

Sorkin LS, Puig S (1996) Neuronal model of tactile allodynia produced by spinal strychnine: effects of excitatory amino acid receptor antagonists and a μ-opiate receptor agonist. Pain 68:283–292.

Spruston N, Johnston D (1992) Perforated patch-clamp analysis of the passive membrane properties of three classes of hippocampal neurons. J Neurophysiol 67:508–529.

Spruston N, Jaffe DB, Johnston D (1994) Dendritic attenuation of synaptic potentials and currents: the role of passive membrane properties. Trends Neurosci 17:161–166.

Takahashi T, Momiyama A (1991) Single-channel currents underlying glycinergic inhibitory postsynaptic responses in spinal neurons. Neuron 7:965–969.

Takahashi T, Momiyama A, Hirai K, Hishinuma F, Akagi H (1992) Functional correlation of fetal and adult forms of glycine receptors with developmental changes in inhibitory synaptic receptor channels. Neuron 9:1155–1161.

Thompson SM, Gahwiler BH (1992) Effects of the GABA uptake inhibitor tiagabine on inhibitory synaptic potentials in rat hippocampal slice cultures. J Neurophysiol 67:1698–1701.

Todd AJ, Spike RC (1993) The localization of classical transmitters and neuropeptides within neurons in laminae I-III of the mammalian spinal dorsal horn. Prog Neurobiol 41:609–645.

Todd AJ, Sullivan AC (1990) Light microscope study of the coexistence of GABA-like and glycine-like immunoreactivities in the spinal cord of the rat. J Comp Neurol 296:496–505.

Todd AJ, Spike RC, Chong D, Neilson M (1995) The relationship between glycine and gephyrin in synapses of the rat spinal cord. Eur J Neurosci 7:1–11.

Todd AJ, Watt C, Spike RC, Sieghart W (1996) Colocalization of GABA, glycine, and their receptors at synapses in the rat spinal cord. J Neurosci 16:974–982.

Todd AJ, Spike RC, Polgár E (1998) A quantitative study of neurons which express neurokinin-1 and somatostatin sst2a receptor in rat spinal dorsal horn. Neuroscience 85:459–473.

van den Pol AN, Gorcs T (1988) Glycine and glycine receptor immunoreactivity in brain and spinal cord. J Neurosci 8:472–492.

Williams SR, Buhl EH, Mody I (1998) The dynamics of synchronized neurotransmitter release determined from compound spontaneous IPSCs in rat dentate granule neurones *in vitro*. J Physiol (Lond) 510:477–497.

Willis WD (1985) The pain system: the neural basis of nociceptive transmission in the mammalian nervous system. Basel: Karger.

Willis WD (1989) The origin and destination of pathways involved in pain transmission. In: Textbook of pain (Wall PD, Melzack R, eds), pp 112–127. New York: Churchill Livingstone.

Woolf CJ, Fitzgerald M (1983) The properties of neurones recorded in the superficial dorsal horn of the rat spinal cord. J Comp Neurol 221:313–328.

Yaksh TL (1989) Behavioral and autonomic correlates of the tactile evoked allodynia produced by spinal glycine inhibition: effects of modulatory receptor systems and excitatory amino acid antagonists. Pain 37:111–123.

Yoshimura M, Nishi S (1993) Blind patch-clamp recordings from substantia gelatinosa neurons in adult rat spinal cord slices: pharmacological properties of synaptic currents. Neuroscience 53:519–526.

Yoshimura M, Nishi S (1995) Primary afferent-evoked glycine- and GABA-mediated IPSPs in substantia gelatinosa neurones in the rat spinal cord *in vitro*. J Physiol (Lond) 482:29–38.

Zhang ET, Craig AD (1997) Morphology and distribution of spinothalamic lamina I neurons in the monkey. J Neurosci 17:3274–3284.

Zhang ET, Han ZS, Craig AD (1996) Morphological classes of spinothalamic lamina I neurons in the cat. J Comp Neurol 367:537–549.